



Low-frequency acoustics in solid ^4He at low temperature

Yu. Mukharsky, A. Penzev, and E. Varoquaux

CEA-DRECAM, Service de Physique de l'État Condensé, Centre d'Études de Saclay, 91191 Gif-sur-Yvette Cedex, France

(Received 11 August 2009; published 8 October 2009)

The elastic properties of hcp ^4He samples have been investigated using low-frequency (20 Hz to 20 kHz) high sensitivity sound transducers. In agreement with the findings of other workers, most samples studied grew very significantly stiffer at low temperature; Poisson's ratio ν was observed to increase from 0.28 below 20 mK to ~ 0.35 at 0.7 K. The span of the variation in ν varies from sample to sample according to their thermal and mechanical history. Crystals carefully grown at the melting curve show a different behavior, the change in ν taking place at lower T and being more abrupt.

DOI: [10.1103/PhysRevB.80.140504](https://doi.org/10.1103/PhysRevB.80.140504)

PACS number(s): 67.80.bd, 61.72.Hh, 62.20.dj

The prospect that solid ^4He may be a supersolid, with both mechanical rigidity and superflow behavior, is arousing strong renewed interest in its mechanical properties below 0.2 K.¹ The supersolidity features are seen primarily in torsional oscillator (TO) measurements of the moment of inertia, which decreases below ~ 0.2 K or so in a way that cannot be accounted for in the framework of classical mechanics, the so-called “nonclassical rotational inertia” (NCRI) effect.²

In this work, we are concerned primarily with the elastic properties of hcp ^4He below 0.8 K. The velocities and attenuation of sound in solid ^4He have long been known to display anomalies at low temperature. Early studies^{3–8} have attributed these anomalies to the presence of dislocation lines, even in good quality crystals, with typical line densities of $\Lambda \approx 10^6 \text{ cm}^{-2}$ and internodal lengths of the dislocation network $L_N \approx 5 \cdot 10^{-4} \text{ cm}$. Already in these early studies, it was noted that sample preparation greatly influences these properties⁵ and could lead to anomalous values of Λ . Nonetheless, these anomalies have been interpreted in the framework of the usual theory of elasticity;^{7,8} they find a natural explanation in terms of dislocation motion in the framework of the Granato-Lücke theory, as discussed by many authors over the years (see, e.g., Refs. 9–11 and references therein).

The more recent work was directed toward the search of clear-cut quantum effects and, possibly, to a direct manifestation of supersolidity,¹² which is now thought to be found in TO measurements.¹³ The anomalies in the shear compressibility are possibly related to those in TO experiments, a possible linkage that makes the subject matter of an ongoing debate.^{9,14} Here we probe directly the low-frequency elastic properties of solid ^4He at unprecedented low levels of strain in the solid ($\epsilon_{zz} < 10^{-10}$) down to below 20 mK in an attempt to test the stress-strain relation for extremely small perturbations and at very low temperature.

The experimental cell consists of a brass cylinder with internal diameter $\Phi_{\text{ID}} = 15 \text{ mm}$, height $h = 20.7 \text{ mm}$, and 0.3-mm-thick walls, immersed in the main body of the sample container, which can be cooled to below 20 mK by a ^3He - ^4He dilution refrigerator. A broadband piezoelectric transducer, made of 12 layers of a PVDF film folded on itself and located at the bottom of the cell, can induce a displacement of the solid helium at frequencies from the subaudio range to above 20 kHz. The resulting strain field can be

detected at the top of the resonator by an ultrasensitive displacement sensor. The sensor consists of a flexible Kapton membrane with a superconducting coating, the position of which is read by an electrodynamic circuit with a dc superconducting quantum interference device amplifier to a resolution in excess of 10^{-15} metre .

The gap between the flexible diaphragm and the backplate in which the superconducting sensing coil is embedded, is quite narrow ($\sim 300 \text{ }\mu\text{m}$). If a pressure P_{el} is applied by the diaphragm (here an electrostatic force) to the solid in the gap, the response is expressed by the following stress-strain relation:¹⁵

$$\sigma_{zz} = P_{\text{el}} = 3K[(1 - \nu)/(1 + \nu)]\epsilon_{zz} = M\epsilon_{zz}. \quad (1)$$

Equation (1), where K is the bulk modulus, ν Poisson's ratio, and M the uniaxial compression modulus, strictly holds for isotropic materials (which hcp ^4He is not). The strain ϵ_{zz} in the flat gap of thickness t equals the measured displacement u_z of the diaphragm divided by t . The strain arising from the side open to the main volume of the cavity is reduced with respect to the thin side by approximately the ratio t/Φ_{ID} of the gap thickness to the cavity diameter.

The piezoelectric transducer, when excited by an ac voltage, generates in the solid a nearly planar displacement along the vertical axis. Away from the cavity acoustic frequencies at which inertia becomes important, and neglecting bulk forces such as arising from gravitation or thermal gradients, the equilibrium displacement field in the cylinder depends only on the displacement at the boundaries and Poisson's ratio ν .¹⁶

When the drive frequency is increased from the low audio to the kHz range, inertia becomes important and acoustic waves, longitudinal and transverse, can propagate through the sample.¹⁷ Standing waves are then sustained when the acoustic half-wavelength matches the size of the cavity, giving rise to acoustic resonances.

The eigenfrequencies of the axisymmetric modes of a solid elastic cylinder with rigid boundary conditions, which models the acoustic cavity used here, have been studied by Hutchinson.¹⁸ The resonances in the finite cylinder closely track those obtained for waves propagating in the infinite cylinder with displacement clamped at the walls and restricted by periodic boundary conditions (zero displacement)

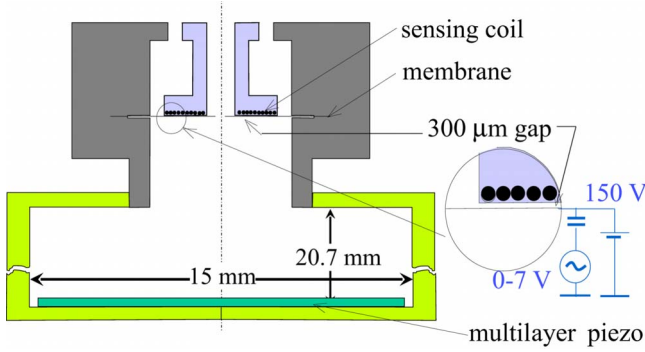


FIG. 1. (Color online) Schematic drawing of the acoustic cell. The displacement gauge is located at the top and the piezoelectric transducer at the bottom. The drawing is approximately to scale, except for the cut that makes it appear shrunk vertically.

at the location of the cavity top and bottom ends. The resonance frequencies for the various modes, normalized to $\omega_0 = 2c_{\perp}/\Phi_{ID}$, $c_{\perp} = [3K(1-2\nu)/2\rho(1+\nu)]^{1/2}$ being the transverse sound velocity (isotropic case), can be expressed in terms of the cylinder aspect ratio h/Φ_{ID} and Poisson's ratio ν . The fundamental mode reduced frequency is equal to $\omega/\omega_0 = \alpha(h/\Phi_{ID}, \nu) = 3.07$ for $h/\Phi_{ID} = 1.38$ and $\nu \sim 0.3$.¹⁹ Direct numerical simulations using the exact cavity geometry yield the same figure to better than 1%.

Thus, the acoustic cell can be operated in three different ways: (1) the variation of uniaxial compression in the displacement sensor gap; (2) that of the transverse velocity (that is, of shear modulus) in the acoustic cavity by the resonance frequency of the fundamental mode; and (3) a direct, albeit less precise, check on the variation of ν in the cavity by the diaphragm response to a quasistatic (70 Hz) actuation of the piezo (Fig. 1). Typical results for measurements (1) and (2) are shown on Figs. 2 and 3 for several samples. These results depend, apart from the cavity geometry, on two quantities, the bulk modulus divided by the density K/ρ and Poisson's ratio ν . Since no pressure variation is recorded when the sample is cooled at constant volume the bulk modulus K remains constant. Its value is known from the phase diagram and from sound velocity measurements.²⁰

The solid ^4He samples have been obtained by the two conventional methods. With the blocked capillary (BC) method, helium is solidified by filling the cell to a given density (or a given pressure, usually 56 bar here), cooled through complete freezing, and then further down in temperature, the quantity of helium in the cell remaining constant because the solid formed in the filling capillary makes an immovable plug at low temperature. This method is used to make samples with densities higher than the density close to melting but subsequent cooling induces thermal stresses that usually damage the crystal. To obtain crystals with lower internal stress, the solid can be grown at low temperature by feeding liquid into the cell at constant temperature (CT), producing samples with a density close to that at melting. Solid ^4He is mechanically fragile: defects can be created by mild mechanical shocks and high intensity sound bursts. The samples were grown from industrial grade helium gas, which contains between 0.1 (as measured in recycled gas) to 0.3

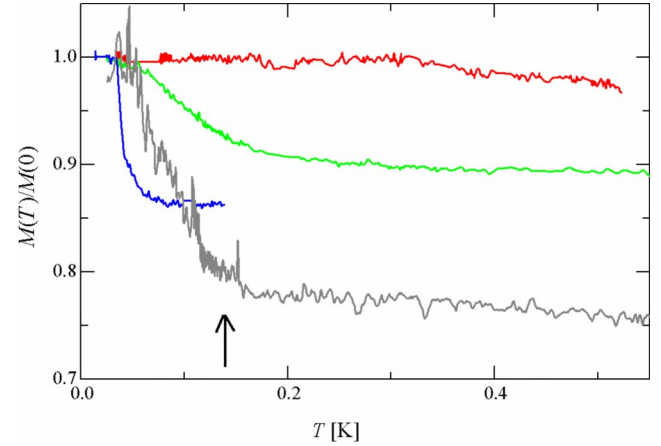


FIG. 2. (Color online) Reduced uniaxial compression modulus $M(T)/M(0.03)$ in terms of the temperature, in kelvin. The curves that extend to above 0.55 K pertain to a typical BC sample at a molar volume of 20.45 cm^3 subjected to different thermal histories (bottom curve, fast cooling, top curve, slow cooling followed by rapid warming to 1.05 K), the two remaining curves to two CT samples, grown at 0.8 K (top) and 1.1 K (truncated at 0.15 K) and slowly cooled. The arrow marks the curve break referred to in the text.

ppm (nominal from the well tap) of ^3He impurities. Upon thermal cycling, crystals may split into crystallites with different orientations, break and regrow, the dislocation line density may either decrease or increase, the ^3He impurities diffuse about onto lower density regions—grain boundaries,

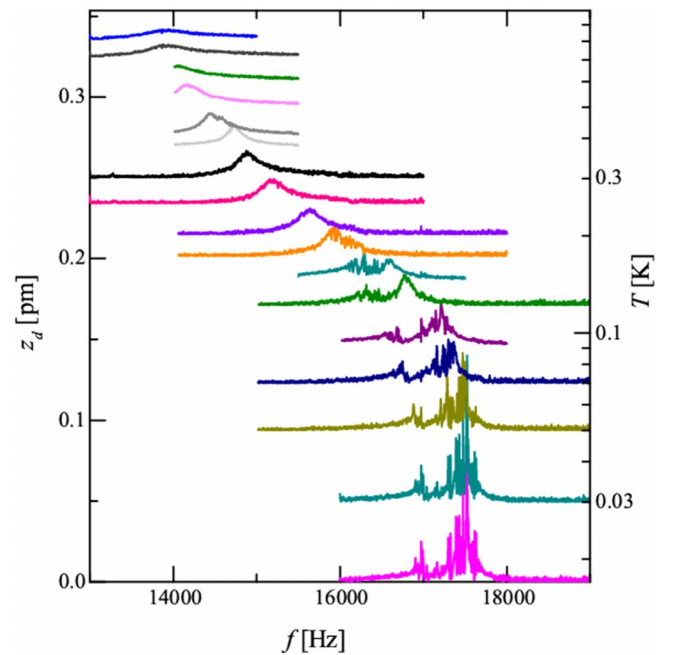


FIG. 3. (Color online) Acoustic spectra at various temperatures for a QC sample with molar volume 20.45 cm^3 ; left y axis, relative diaphragm displacement z_d in picometers; right y-axis, temperature in Kelvin on a logarithmic scale; x axis, frequency in Hertz. Below 200 mK, the resonance line splits and develops wiggles; a satellite also develops to the left of the main peak.

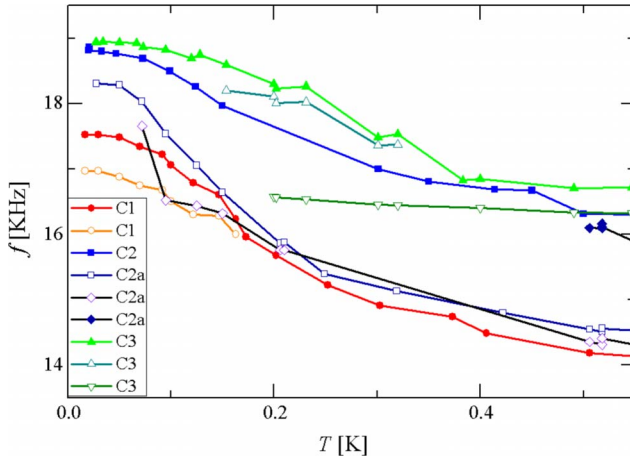


FIG. 4. (Color online) Acoustic resonance peak frequency vs temperature for several BC samples: C1, quenched, same as in Fig. 3; C2, 20.63 cm^3 per mole, slowly cooled, C2a, after thermal shock; C3, 20.06 cm^3 per mole. This last sample exhibits three resonance peaks, one of which disappears below ~ 0.2 K.

liquid inclusions, and, quite importantly here, on dislocation cores, providing pinning sites.

The temperature variation of the uniaxial compression modulus M , given by the diaphragm displacement under a given applied force, is shown in Fig. 2 for a BC sample of molar volume 20.45 cm^3 , determined by an ancillary quartz resonator in the liquid phase, and different cooling rates, as well as two CT samples grown at different temperatures (0.8 and 1.1 K). The CT ($T=1.1$ K) sample shows a marked drop below 50 mK, the other CT ($T=0.8$ K) sample shows no variation below ~ 0.3 K down to 33 mK. Most samples however do show a stiffening at low temperatures that varies in overall magnitude and onset temperature according to their thermal and mechanical history. These observations fully vindicate previous studies,^{3,5-9} including the markedly different behaviors of CT samples.⁷

When the drive frequency is scanned, using the piezo as a transmitter and the diaphragm as a microphone, the fundamental resonance frequency yields, in a first approximation as discussed above, the change in the shear modulus $G_{\text{eff}} = 3K(1-2\nu)/2(1+\nu) = \rho c_{\perp}^2$ with temperature. An example of such scan is given in Fig. 3; the frequency of the resonance peak decreases by 20% from 17 to 717 mK, which implies that the effective shear modulus G_{eff} is divided by 1.58 upon warming.

The resonance frequencies in different samples are shown in terms of the temperature in Fig. 4. As for the uniaxial compression modulus, the frequency shifts are markedly sample dependent. The variations in the low-temperature limit for samples grown at the same density reflect variations in the crystal orientation and (or) its splitting into several grains, or also the presence of residual stress and pressure inhomogeneities. We have no control over the actual crystal orientation although, on occasions, it can be inferred unambiguously from the observed fundamental frequency.

It is noteworthy that the CT sample that showed no variation in M in Fig. 2 exhibits no frequency shift. Uniaxial compression applies shear in two different planes, at least

one of which is not parallel to the glide plane of the dislocations. The acoustic resonance generates strains in all directions. Dislocations, if present and unpinned, should have contributed to the total strain, which they did not.

In most samples, two different regimes appear below and above the temperature T^* around which the frequency shifts at the fastest rate (~ 200 mK in Fig. 3), which is also the temperature at which the resonance amplitude goes through a minimum. Contrarily to other work,⁹ we do not observe a narrowing of the resonance line, but a splitting into several resonances, or wiggles, below T^* . This splitting is more pronounced at the lowest temperature, where the crystal is stiffest and intrinsic damping lowest. On occasions, distinct, weak, resonance peaks also show up several hundreds of Hz above or below the main resonance line. Both features, which can be seen in Fig. 3, appear in the linear-response regime. Their origin is unknown but they reveal that the resonance line is inhomogeneously broadened at $T \geq T^*$ and partially resolved below, presumably because damping decreases.²¹ The fundamental mode depends on some coarse-grained *average* of the density and elastic properties of the medium in the acoustic cavity and does not probe inhomogeneities or localized defects. We believe that the splitting and the satellite lines arise from the existence of additional, macroscopic, degrees of freedom within the solid sample as, for instance, a condensate fraction, or a dislocation network collective motion.

At higher drive levels, nonlinear effects appear, notably frequency pulling that tends to push the resonance frequency back to its high-temperature value. The drive amplitude at which this effect sets in depends on temperature; it goes through a minimum around 100 to 200 mK. The value of the strain is $\sim 10^{-9}$, an order of magnitude lower than the threshold reported in Ref. 11. It should be noted that the corresponding displacement at its maximum, at the center of the cavity, is exceedingly small, less than one tenth of the width of the Peierls valley.

From the low T limit of the resonance frequency in Fig. 3, $\omega/2\pi = 17.5$ kHz, and $\alpha = 3.07$, we find, using for the value of the bulk compression modulus at a molar volume of 20.65 cm^3 , $K = 275$ bar,²² a value for Poisson's ratio of 0.28 at 0.02 K, not much different from the value obtained by high-frequency sound measurements,¹⁹ climbing back to 0.36 at 0.7 K with the appropriate value of α (3.20). A similar variation is obtained from the change in uniaxial compression modulus in Fig. 2.

Most of the features reported here find a natural explanation in terms of dislocation motion in the framework of the Granato-Lücke theory as used by many authors over the years (see, e.g., Refs. 3-7, 9, and 11) and may also be related to the anomalies in the TO experiments as discussed in Refs. 9 and 14. Other features do not. The behavior of the CT samples, showing a more abrupt (or else, very little) change in G_{eff} at lower T requires a like-sudden change (or lack of) in dislocation pinning. Such behaviors have also been observed in TO experiments on the NCRI fraction in good quality samples.²³ Sometimes, the T dependence of G_{eff} shows an abrupt change of slope, as can be seen in Fig. 2 for the fast-cooled BC sample around $T = 0.14$ K. Such breaks in the T dependence are not expected in the dislocation line

model that relies on the condensation of ^3He impurities on dislocation cores and leads to a more rounded variation^{5,6} such as that obtained after warming the sample to 1.05 K.

Let us nonetheless interpret the drastic change in elastic properties observed here in terms of the strain induced by dislocations, following Paalanen *et al.*⁷ and using their expression

$$G/G_{\text{eff}} = 24R(1 - \nu)\Lambda L^2/\pi^3 + 1, \quad (2)$$

R depending on the orientation between the local displacement vector and the c -axis of the crystal. Assuming equal weight between longitudinal and transverse motions, $R \leq 1/4$ and using our result $G/G_{\text{eff}} = 1.58$ and $\nu = 0.3$, we find $\Lambda L^2 \geq 4.2$. This value greatly exceeds that found experimentally by Iwasa *et al.*⁵ (0.21) and justified theoretically by them for the hcp lattice, and is also larger than that quoted by Paalanen *et al.* (≈ 2.0).⁷ The stiffness of hcp ^4He decreases

very markedly above ~ 0.1 – 0.2 K in impure, quenched BC crystals, above ~ 50 – 70 mK in better quality CT crystals. The corresponding value of ΛL^2 is anomalously large: dislocations seem to proliferate and creep over all the space available to them even for extremely small strains as if Peierls' barrier was irrelevant.

In this work we have established the following: (1) Poisson's ratio recovers at low T its value derived from high-frequency sound propagation, which is close to its intrinsic value as advocated by Day *et al.*;⁹ (2) the large value of ΛL^2 in some samples points toward the existence of a fractured, highly disorganized dislocation network; and (3) Peierls' barrier does not hinder dislocation motion, hinting that dislocations may be rough on an atomic scale.

We thank Sébastien Balibar, Giulio Biroli, Jean-Philippe Bouchaud, and Francesco Zamponi for stimulating discussions from which we have greatly benefitted.

¹N. Prokof'ev, Adv. Phys. **56**, 381 (2007); S. Balibar and F. Caupin, J. Phys.: Condens. Matter **20**, 173201 (2008); D. E. Galli and L. Reatto, J. Phys. Soc. Jpn. **77**, 111010 (2008).

²A. Leggett, Phys. Rev. Lett. **25**, 1543 (1970).

³R. Wanner, I. Iwasa, and S. Wales, Solid State Commun. **18**, 853 (1976).

⁴V. L. Tsymbalenko, Sov. Phys. JETP **45**, 989 (1977).

⁵I. Iwasa, K. Araki, and H. Suzuki, J. Phys. Soc. Jpn. **46**, 1119 (1979).

⁶F. Tsuruoka and Y. Hiki, Phys. Rev. B **20**, 2702 (1979).

⁷M. A. Paalanen, D. J. Bishop, and H. W. Dail, Phys. Rev. Lett. **46**, 664 (1981).

⁸Y. Hiki and F. Tsuruoka, Phys. Rev. B **27**, 696 (1983).

⁹J. Day, O. Syshchenko, and J. Beamish, arXiv:0903.1269 (unpublished), and references therein.

¹⁰J. Beamish, J. Phys. (Paris) **46**, C10-147 (1985).

¹¹O. Syshchenko, J. Day, and J. Beamish, J. Phys.: Condens. Matter **21**, 164204 (2009).

¹²J. M. Goodkind, Phys. Rev. Lett. **89**, 095301 (2002), and references therein.

¹³E. Kim and M. Chan, Science **305**, 1941 (2004).

¹⁴A. C. Clark, J. D. Maynard, and M. H. W. Chan, Phys. Rev. B **77**, 184513 (2008).

¹⁵L. Landau and E. Lifshitz, *Theory of Elasticity* (Pergamon Press,

London, 1959), Chap. I, p. 15.

¹⁶See [15](#), Sec. 7.

¹⁷The present cell is an improved version of that used for the work reported by Mukharsky, Avenel, and Varoquaux, J. Low Temp. Phys. **148**, 689 (2007). The increase in stiffness at low temperature was already observed then.

¹⁸J. Hutchinson, J. Acoust. Soc. Am. **42**, 398 (1967).

¹⁹Assuming the longitudinal and mean transverse sound velocities to be $c_{\parallel} = 460$ m/s and $c_{\perp} = 240$ m/s for 21.0 cm³/mole and 1.3 K [R. H. Crepeau, O. Heybey, D. M. Lee, and S. A. Strauss, Phys. Rev. A **3**, 1162 (1971)], $\nu = (c_{\parallel}^2/2c_{\perp}^2 - 1)/(c_{\parallel}^2/c_{\perp}^2 - 1) = 0.31$; Tsuruoka and Hiki (Ref. [6](#)) reported a value of 0.294 at 20.5 cm³/mole.

²⁰D. Greywall, Phys. Rev. A **3**, 2106 (1971).

²¹It is unlikely that the wiggles would have arisen from some unsuspected experimental artefact such as a parasitic resonance. The wiggles are not seen in liquid where lines are sharp. They come in different forms with different solid samples. All samples except the CT sample grown at 0.8 K show a split fundamental resonance.

²²From Fig. 17 in Ref. [20](#). The density in the cavity can be less than that in the main cell for quenched crystals.

²³A. C. Clark, J. T. West, and M. H. W. Chan, Phys. Rev. Lett. **99**, 135302 (2007).